Bull Volcanol (1996) 58:144–162

ORIGINAL PAPER

J. E. Gardner · R. M. E. Thomas · C. Jaupart
S. Tait

Fragmentation of magma during Plinian volcanic eruptions

Received: 19 April 1995 / Accepted: 3 April 1996

Abstract The ratio of the volume of vesicles (gas) to that of glass (liquid) in pumice clasts (V_G/V_L) reflects the degassing and dynamic history experienced by a magma during an explosive eruption. V_G/V_L in pumices from a large number of Plinian eruption deposits is shown here to vary by two orders of magnitude, even between pumices at a given level in a deposit. These variations in V_G/V_L do not correlate with crystallinity or initial water content of the magmas or their eruptive intensities, despite large ranges in these variables. Gas volume ratios of pumices do, however, vary systematically with magma viscosity estimated at the point of fragmentation, and we infer that pumices do not quench at the level of fragmentation but undergo some post-fragmentary evolution. On the timescale of Plinian eruptions, pumices with viscosities $<10^9$ Pa s can expand after fragmentation, as long as their bubbles retain gas, at a rate inversely proportional to their viscosity. Once the bubbles connect to form a permeable network and lose their gas, expansion halts and pumices with viscosities $<10^5$ Pa s can collapse under the action of surface tension. Textural evidence from bubble sizes and shapes in pumices indicates that both expansion and collapse have taken place. The magnitudes of expansion and collapse, therefore, depend critically on the timing of bubble connectivity relative to the final moment of quenching. We propose that bubbles in different pumices become connected at different times throughout the time span between fragmentation and quenching. After accounting for these effects, we derive new information on the fragmentation process from two characteristics of pumices. The most important is a relatively constant minimum value of V_G/V_L of ~ 1.78 (64 vol.% vesicularity) in all samples with viscosities $>10^5$ Pa s. This value is independent of magma composition and thus reflects a property of the eruptive mechanism. The other characteristic is that highly expanded pumices (>85 vol.% vesicularities) are common, which argues against overpressure in bubbles as a mechanism for fragmenting magma. We suggest that magma fragments when it reaches a vesicularity of ~ 64 vol.%, but only if sheared sufficiently strongly. The intensity of shear varies as a function of velocity in the conduit, which is related to overpressure in the chamber, so that changes in overpressure with time are important in controlling the common progression from explosive to effusive activity at volcanoes.

Key words Magma fragmentation · Pumice vesicularity · Volcanic eruptions · Bubble connectivity

Editorial responsibility: S. Carey

James E. Gardner[1] (✉) · Richard M. E. Thomas[2]
Claude Jaupart · Steve Tait
Laboratoire de Dynamic des Systèmes Géologiques,
Institut de Physique du Globe, 4 place Jussieu,
F-75252 Paris cédex 05, France

Present addresses:
[1]GEOMAR, Abteilung Vulkanologie,
Wisschofstrasse 1–3, D-24148 Kiel, Germany
Fax: (49) 431 600 2924
e-mail: jgardner@geomar.de

[2]Cartography Ltd., 47 City Road, Cambridge, England

Introduction

The amount of gas bubbles in volcanic pumice clasts – quenched, vesicular fragments of magma – reflects the degassing and dynamic history experienced by magma during explosive eruptions. Sparks (1978) suggested that magma disrupts when vesicularity reaches a value of approximately 75 vol.%, because of overpressure in bubbles. Although many studies have since found that the mean vesicularity of pumice is commonly around 75 vol.% (Heiken and McCoy 1984; Carey and Sigurdsson 1987; Houghton and Wilson 1989; Wilson and Sparks 1989; Gardner et al. 1991; Orsi et al. 1992; Klug and Cashman 1994a), the idea that pumices have vesicularities tightly clustered around 75 vol.% is misleading. This is because the use of vesicle volume fraction (vesicularity) as the characteristic measure masks differences in gas volume at high void fractions, as does any percentage quantity when one component dominates. If the volume of vesicles (gas) is ratioed directly to the volume of glass (liquid) (V_G/V_L), we find that, for example in the Taupo Plinian deposit, pumices with vesicularities of 65 and 83 vol.%, considered a small spread in vesicularity (Houghton and Wilson 1989), really have a difference in gas volume of approximately 2.6 times. Large differences in gas volumes are also present among pumices in the Minoan, Bishop tuff, and Mount St. Helens Plinian deposits (Thomas et al. 1994; Klug and Cashman 1994a). The volume of gas thus varies greatly in the clasts ejected by Plinian eruptions.

The fact that pumices produced in magmatic eruptions have vastly different gas volumes raises the questions of whether such differences represent the vesicularity of magma when it fragments and, if not, what they do represent. These questions bear directly on the process of fragmentation, because V_G/V_L is related to the mass ratio of exsolved gas to melt (M_G/M_L) through the ratio of densities of gas and melt. If, for example, the pressure at which pumice quench remains constant during an eruption, then variations in V_G/V_L reflect changes in the mass fraction of gas, whereas if the mass fraction of gas were constant, changes in pressure are implied. In previous studies of vesicularity, the key assumption made is that pumices reflect the state of the magma when it fragments, which relies on an unspecified process which quenches instantaneously the pieces of vesicular magma as they form. This implies that either different batches of Taupo magma exsolved very different amounts of gas or the pressure at the fragmentation level varied greatly. Recent physical modeling suggests, however, that pumices can deform after the magma disrupts, thus modifying their vesicularities significantly (Thomas et al. 1994). Textural evidence on the vesicle sizes in pumices erupted during the 1980 eruption of Mount St. Helens, for example, appears to support the idea that pumices can expand (Klug and Cashman 1994a). The wide ranges in V_G/V_L in pumices may thus represent heterogeneities in the evolution of gas volume after fragmentation.

To constrain the relative importance of the different potential sources for variable V_G/V_L requires that the deposits studied be produced by the same eruptive mechanism and that the magmas erupted have properties which cover the widest possible ranges. We carried out a study restricted to pumices produced in Plinian eruptions, in which fragmentation is from disruption by magmatic volatiles. In total, we measured the vesicularities of 2615 pumice clasts from 13 Plinian eruptions. The eruptions studied also tapped magmas which range in composition from basalt to high-silica rhyolite, and have very different crystal contents, temperatures, and water contents (Table 1). These differences allow the influence of pre-eruptive heterogeneities to be investigated. In addition, the large range in composition also leads to a wide range in viscosity (many orders of magnitude), which allows the influence of postfragmentation processes to be studied, because these are directly controlled by viscosity.

A key feature of our approach is to evaluate these data in the context of a physical model of the evolution of clasts after fragmentation. The enormous range of magma viscosities involved means that we are able, ultimately, to view the data as a function of this variable alone because other model parameters vary little in comparison. The overall logic of the data in the context of this model provide a powerful constraint on the origins of the variations in V_G/V_L and, hence, on the fragmentation process.

Samples and analytical techniques

We studied 13 different deposits of Plinian eruptions (Table 1). In most cases composition and eruptive intensity have been determined previously; see Table 1 for references. Here, we summarize our samples and the analytical techniques employed to determine their vesicularities. All samples consisted of randomly selected clasts, 2–8 cm in size, which are representative of the deposits (Table 2).

Pumices were collected from 40- to 70-cm-thick levels in the Plinian deposits of the Minoan (Fig. 1a), Upper Scoria 1 (Fig. 1b), and Middle Pumice (Fig. 1c) sequences erupted from Santorini volcano, Greece. In addition, 149 large pumices which range in size from 8 to 32 cm were collected from the Minoan and Middle Pumice deposits. Although evidence exists for phreatomagmatic activity during parts of the Minoan and Upper Scoria 1 eruptions (Wilson and Houghton 1989; Mellors and Sparks 1991), our samples come from the "dry" Plinian stages of these eruptions, when fragmentation resulted from magmatic volatiles. Our Minoan samples contain only rhyodacitic pumices, which make up >99% of the deposit (Druitt et al. 1989). The Middle Pumice deposit is zoned compositionally from dacite to silicic andesite (Druitt et al. 1989), but our samples contain only the dominate pumice type in the base and top levels. Discharges for the Upper Scoria 1 and Middle Pumice eruptions have not been quantified, so as a preliminary estimate, we measured the five largest lithic clasts from the same levels in the deposits as our samples and estimated discharge using the method of Carey et al. (1990). Reverse-size grading indicates that discharge increased during both eruptions (Table 1).

We sampled the 79 A.D. deposit erupted from Vesuvius (Fig. 1d) at the Boscoreale locality of Sigurdsson et al. (1985). This deposit is stratified from evolved "white" phonolite to "gray" tephric phonolite, divided by a sharp boundary. Dark and light gray pumices occur in the lower part of the gray tephra, but differ only in density. The samples with these two pumice types (VES93-4 and VES93-6) contain them in their relative abundances. Late in the Vesuvius eruption, phreatomagmatic activity became important (Sigurdsson et al.

Table 1 Magma Compositions and Eruptive Dynamics of Plinian Eruptions

Eruption[a]	Bulk[b]	Melt[b]	Crystals (vol.%)	Temp[c] (°C)	Water[d] (wt.%)	log Visc[e] (Pa s)	log MDR[f] (kg/s)	Volume[g] (km^3)	References[h]
Bishop tuff	HSR	HSR	10	750	5.5	4.8	9.0	~80	1, 2, 3, 4
Vesuvius (79 A.D.)									
White	P	P	18	830	4.7	3.5	7.9	1	5, 6, 7
Gray	TepP	P	27	870	3.5	4.3	8.0	2.6	
Mount St. Helens									
T	D	R	31	890	4.6	4.6	7.0	0.4	8, 9
Wn	D	R	27	850	4.8	5.7	7.7	2	8, 9
Pu	D	R	43	870	4.3	6.1	6.3	0.2	8, 9
Yn	D	R	37	780	6.4	5.3	8.0	4	8, 9
Canary Islands									
Montaña Blanca	P	P	5	850	3.0	4.0	7.2	0.2	10, 11
Azores									
Fogo	P	P	5	850	2.9	4.1	8.0	1.7	11, 12
Newberry	R	R	0	–	–	–	6.0	0.1	4, 13
Santorini									
US 1	A	A	14	1000	3.2	2.5	7.0	–	11, 14, 15
MP (base)	D	D	16	890	5.6	3.4	7.1	–	11, 14
MP (top)	SA	SA	15	–	–	–	7.3	–	
Minoan	RD	R	15	870	6.2	4.0	8.4	2	11, 12, 16, 17
Masaya									
Fontana	B	B	5	1200	2.0	1.0	8.2	3.4	11, 18

[a] Tephra layers studied. Bishop tuff data are for the Plinian phase of that eruption. Vesuvius White and Gray refer to two magma types tapped during the eruption; US 1 = Upper Scoria 1; MP = Middle Pumice

[b] Bulk and melt compositions; B = basalt, A = andesite, SA = silicic andesite, TepP = tephritic phonolite, P = phonolite, D = dacite, RD = rhyodacite, R = rhyolite, HSR = high-silica rhyolite

[c] Temperatures calculated from phase equilibria. Temperature for Bishop tuff was calculated using scheme of Anderson and Lindsley (1988). Yn magma is graded thermally by ~25 °C; the average is used here. Temperatures for Montaña Blanca, Fogo, Upper Scoria 1, and Fontana are assumed

[d] Pre-eruptive water content dissolved in melt. Water content for Fontana is assumed

[e] Magmatic viscosity calculated from model of Shaw (1972), and modified for crystallinity (Marsh 1981). Viscosity of Fontana is assumed

[f] Peak magma discharges

[g] Volume (dense-rock equivalent) for Plinian phase of each eruption

[h] 1 Hildreth (1977); 2 Anderson et al. (1989); 3 Gardner et al. (1991); 4 Gardner, Sigurdsson, and Carey (unpublished data); 5 Cornell (1987); 6 Carey and Sigurdsson (1987); 7 Barberi et al. (1981); 8 Carey et al. (1995); 9 Gardner et al. (1995a, b); 10 Ablay et al. (1995); 11 this study; 12 Carey and Sigurdsson (1989); 13 Sherrod and MacLeod (1979); 14 Druitt et al. (1989); 15 Mellors and Sparks (1991); 16 Sigurdsson et al. (1989); 17 M. Rutherford (pers. commun. 1995); 18 Williams (1983)

1985; Barberi et al. 1989), yet our samples come from only the "dry" Plinian stages of the eruption.

The basaltic Fontana deposit, erupted from Masaya volcano, Nicaragua, was sampled at two localities, 7 km (Fig. 1e) and 16 km from vent (Table 2). Williams (1983) showed that the variation in lithic sizes in this deposit is very similar to that of the 1902 Santa Maria eruption, which had a column height of approximately 34 km (Carey and Sparks 1986). This suggests that the Fontana eruption column was similar in size and, thus, discharge was $\sim 1.6 \times 10^8$ kg s^{-1}, based on theoretical curves given in Sparks (1986). This intensity agrees well with the 3.4 km^3 of magma erupted (Williams 1983), based on the correlation of intensity with volume of 45 Plinian eruptions (Carey and Sigurdsson 1989).

Bulk samples were collected from eight deposits, none of which exhibit evidence for phreatomagmatic activity. These samples are composed of pumices taken from the full thickness of the deposits at one to three localities. Pumices were collected from four deposits erupted from Mount St. Helens (USA): T (age of 1800 A.D.), Wn (1480 A.D.), Pu (~2700 y.b.p.), and Yn (3500 y.b.p.). All of these pumices are dacitic, composed of variable amounts of rhyolitic glass and crystals (Table 1). The 2020 y.b.p., crystal-poor, phonolitic deposit of Montaña Blanca, Tenerife, was sampled at three localities: 2, 4, and 6 km from vent. A few reticulites with vesicularities up to 98 vol.% were found, but are not included in the population statistics because they make up only ~0.00025 vol.% of the deposit, based on the amount of deposit sampled. Their presence is included in the Discussion. A sample of holohyaline, rhyolitic pumices was collected from the ~1300 y.b.p. deposit from Newberry volcano (USA) from a 3.2-m-thick section located 4.5 km from vent. Finally, individual pumices from the Plinian phase of the Bishop tuff eruption measured for density by Gardner et al. (1991) are included, and a sample of 174 pumices from the 4600 y.b.p. eruption of Fogo, Azores (Walker and Crosdale 1973), is also included.

Table 2 Summary of Gas Volume Ratio Measurements for Plinian Eruptions

Eruption[a]	Sample[b]	N[c]	Mean[d]	High[d]	Low[d]	SD[e]	Water[f] (wt.%)	log Visc[g] (Pa s)
Bishop tuff	–	25	2.70	3.50	1.70	0.46	1.9	8.0
Vesuvius (79 A.D.)								
White	VES93-1	100	3.98	6.62	1.38	0.90	2.0	4.9
	VES93-3	100	3.70	6.46	1.96	0.84		
Gray	VES93-4	166	1.97	4.00	0.89	0.63		
	VES93-6	131	3.38	6.34	1.49	1.05	1.6	5.4
	VES93-8	100	3.62	7.06	1.68	1.00		
Mount St. Helens								
T	–	12	4.44	6.83	2.08	1.24	1.7	6.6
Wn	–	49	3.41	5.05	1.54	0.74	2.0	7.3
Pu	–	35	4.09	6.34	1.48	1.08	1.8	7.8
Yn	–	35	2.88	5.49	2.12	0.56	1.9	8.7
Teide								
Montaña Blanca	–	300	4.47	12.61	0.589	1.44	1.7	4.7
Azores								
Fogo	–	174	4.75	13.61	1.89	1.86	1.3	5.1
Newberry	–	49	3.16	4.88	1.80	0.73	–	–
Santorini								
US 1	US193-1	90	1.42	3.92	0.132	0.68	2.1	3.4
	US193-6	100	2.42	4.38	0.521	0.76		
	US193-7	100	1.70	4.05	0.221	0.83	2.1	3.4
	US193-11	100	2.65	4.95	0.589	0.84		
MP	MP93-12	100	4.46	13.71	1.60	1.89	2.1	5.4
	MP93-16	100	2.66	5.27	0.788	1.01	–	–
Minoan	MIN93-10	100	3.87	6.30	1.60	1.01	2.2	6.7
	MIN93-12	100	4.25	8.91	2.59	1.15		
Masays								
Fontana	SAM9.1	100	2.22	4.69	0.296	0.94	–	2.0
	SAM9.5	100	2.31	5.63	0.160	0.83		
	SAM9.7	100	1.81	3.54	0.136	0.74		
	SAM1.1	100	2.28	4.74	0.472	0.84		

[a] See Table 1 for eruption descriptions. Two stratigraphic sections were measured for US 1 at 5 and 7 km from vent; the closer locality is listed first
[b] See Fig. 1 for stratigraphic position. A sample stratigraphically equivalent to SAM9.1 was sampled from the Fontana deposit at a locality 16 km from vent (SAM1.1)
[c] Number of pumices measured for deposit or sample level
[d] Average, maximum, and minimum values for gas volume ratios from deposit or sample level
[e] Standard deviation of gas volume ratios
[f] Water contents dissolved in melt after exsolution of enough gas to produce minimum volume ratios, assuming that bubbles and melt remain in equilibrium during ascent (see text for discussion)
[g] Viscosity calculated using degassed water contents and the model of Shaw (1972), modified for crystallinity (Marsh 1981). Viscosity for degassed Fontana magma is assumed

Pumice densities and vesicularities

A total of 2615 pumices were measured for their densities using a water-displacement method. First, pumices were cleaned, dried, and weighed, and then immersed in distilled water. After saturating with water, each pumice was placed in a pycnometer which was then filled with distilled water to a constant level and weighed. Pumices were then removed from the pycnometer and weighed wet. The volume of each pumice was calculated from the weights of the pycnometer with and without the pumice and the wet and dry weights of the pumice. Replicate measurements of pieces of pumices machined into known volumes indicate that accuracy and precision is approximately ±3%. Pumice density was then calculated from dry weight and volume. Densities of the Mount St. Helens pumices were determined using a similar method (Gardner 1993). The densities of large pumices from the Minoan and Middle Pumice deposits were measured in the field using a similar technique, except that beakers of known volume were used to measure water displaced by immersion. Pumices from the Newberry deposit were determined using the technique of Gardner et al. (1991).

The vesicularity of each pumice clast was calculated from its density and the densities of glass and crystals in their known proportions. A single value for crystallinity was used to calculate vesicularity for each pumice in a population, although they probably do not contain exactly the same amount of crystals. This has little effect, however, even for pumices with high crystallinities, as shown by 20 pumices from the Mount St. Helens deposits for which crystal contents were determined by chemical mass balance (Table 3). The small differences re-

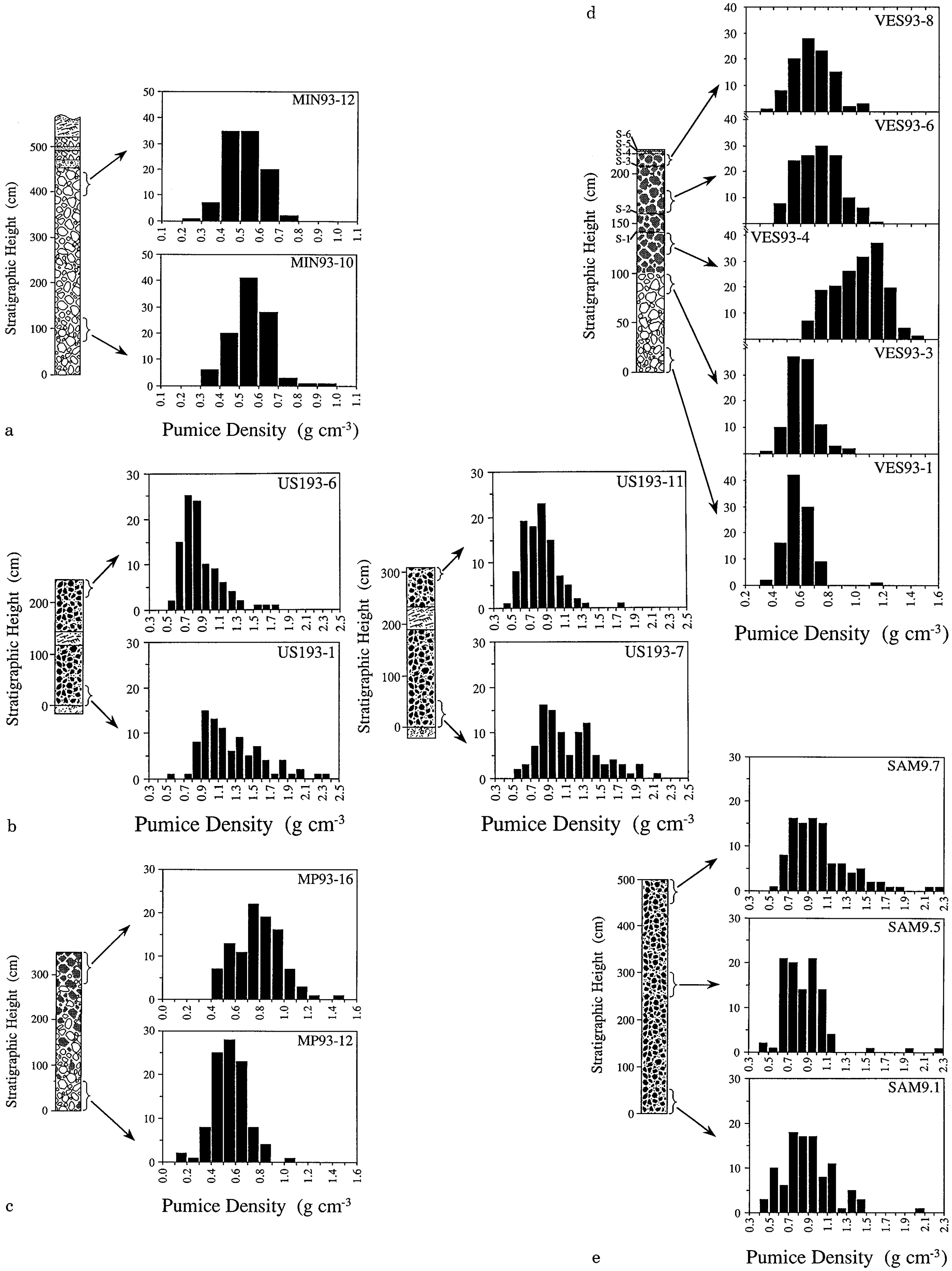
a
b
c
d
e
MIN93-12
MIN93-10
US193-6
US193-1
US193-11
US193-7
MP93-16
MP93-12
VES93-8
VES93-6
VES93-4
VES93-3
VES93-1
SAM9.7
SAM9.5
SAM9.1
S-6
S-5
S-4
S-3
S-2
S-1
Stratigraphic Height (cm)
Pumice Density (g cm-3)

Fig. 1a–e

◀ **Fig. 1** **a** Stratigraphic column of Minoan Plinian deposit showing levels sampled and their histograms of pumice density. Two ash-rich zones are present in the upper part of the deposit at this locality, which is approximately 3 km from vent. **b** Stratigraphic columns of Upper Scoria 1 Plinian deposit showing levels sampled and their histograms of pumice density. Samples were collected at two localities, 5 and 7 km from vent, with the closer locality shown first. There are stratified surge beds located at the base and in the middle of the deposit at both localities. **c** Stratigraphic column of Middle Pumice Plinian deposit showing levels sampled and their histograms of pumice density. The deposit is stratified from dacite (*white*) to silicic andesite (*shaded*). This locality is approximately 7 km from vent. **d** Stratigraphic column of 79 A.D. Vesuvius Plinian deposit showing levels sampled and their histograms of pumice density. The deposit is stratified from evolved phonolite (*white*) to tephritic phonolite (*shaded*), separated by a sharp boundary. At this locality, 7 km from vent, six intra-Plinian surges are found (S levels, following Sigurdsson et al. 1985). **e** Stratigraphic column of Fontana Plinian deposit showing levels sampled and their histograms of pumice density. This locality is approximately 5 km from vent

sult from the relatively small density difference between most crystals and silicate melt and the relatively small abundance of crystals in vesicular pumices.

To better characterize the variations of gas volume in erupting magma, the ratio of gas volume to melt volume for each pumice was calculated from their vesicularities by the following equation:

$$\frac{V_G}{V_L} = \frac{Ves}{1-Ves}\left(\frac{1}{1-m}\right) \tag{1}$$

where V_G is the volume of gas (vesicles), V_L is the volume of melt (glass), Ves is the volume fraction of vesicles and m is the modal fraction of crystals. It can be seen from Eq. (1) that when vesicularity varies between 1 and 99%, V_G/V_L actually varies by more than three orders of magnitude (Fig. 2). The correction for crystallinity allows the gas volume ratio to measure directly the volume of gas relative to the volume of melt from which it exsolved. V_G/V_L was calculated for each pumice using an average value for crystallinity (Table 2). Gas volume ratios calculated using either an average value or individual values differ on average by approximately 4%, which is small compared with the full variations observed (Table 2).

Pre-eruptive water contents

We determined the pre-eruptive water contents of the Montaña Blanca, Fogo, Upper Scoria 1, Middle Pu-

Table 3 Vesicularities and Gas/Melt Volume Ratios of Mount St. Helens Pumices with Individual Modes

Eruption	Pumice	Mode[a] (vol.%)	ρ[a] (g cm^{-3})	Ves (mode)[b] (vol.%)	Ves (average)[b] (vol.%)	V_G/V_L (mode)[c]	V_G/V_L (average)[c]
T	MSH357-1	37	0.73	71.2	71.1	3.92	3.57
	MSH357-2	34	0.54	78.6	78.6	5.56	5.32
	MSH325-1	31	1.03	58.9	59.2	2.08	2.10
				Average: 69.6	Average: 69.6	Average: 3.85	Average: 3.66
				SD: 10.0	SD: 9.8	SD: 1.74	SD: 1.61
Wn	MSH313-1	29	0.89	64.4	64.5	2.41	2.49
	MSH313-2	25	0.78	68.7	68.9	3.09	3.03
	MSH320-1	33	0.85	66.2	66.1	2.92	2.67
	MSH320-3	34	0.80	68.2	68.1	3.25	2.92
	MSH320-4	30	0.65	74.1	74.1	4.09	3.92
				Average: 68.3	Average: 68.3	Average: 3.15	Average: 3.01
				SD: 3.65	SD: 3.65	SD: 0.61	SD: 0.55
Pu	MSH363-2	43	0.68	73.6	73.6	4.89	4.89
	MSH372-1	45	0.63	75.6	75.5	5.63	5.41
	MSH372-3	44	0.80	68.9	68.9	3.96	3.89
	MSH372-13	46	1.18	54.3	54.1	2.20	2.07
				Average: 68.1	Average: 68.0	Average: 4.17	Average: 4.07
				SD: 9.6	SD: 9.7	SD: 1.48	SD: 1.47
Yn	MSH334-1	38	0.86	66.0	66.2	3.13	3.11
	MSH334-2	39	1.04	58.9	59.2	2.35	2.30
	MSH336-4	36	0.82	67.5	67.8	3.25	3.34
	MSH336-6	34	0.99	60.6	61.1	2.33	2.49
	MSH338-1	39	0.86	66.0	66.2	3.18	3.11
	MSH338-3	37	0.74	70.8	71.0	3.85	3.89
	MSH340-4	34	0.82	67.5	67.8	3.15	3.34
	MSH340-6	35	0.99	60.6	61.1	2.37	2.49
				Average: 64.7	Average: 65.1	Average: 2.95	Average: 3.01
				SD: 4.2	SD: 4.1	SD: 0.55	SD: 0.54

[a] Crystal modes from Gardner et al. (1995a); pumice densities from Gardner (1993)

[b] Vesicularities calculated using either known crystal mode (mode) or a single value (average). See Table 1 for values

[c] Gas volume ratios (see Eq. 1) calculated from vesicularities

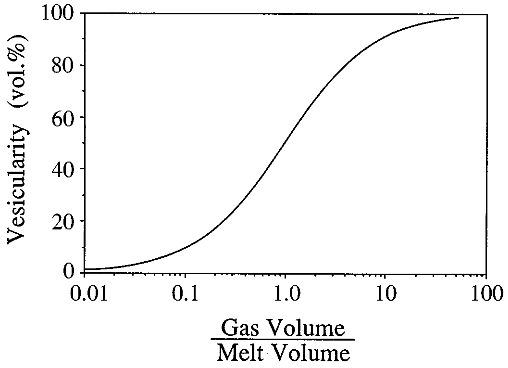

Fig. 2 Scale showing V_G/V_L values which correspond to conventionally reported vesicularities. Note that the change from 1 to 99 vol.% equals more than three orders of magnitude difference in gas volume

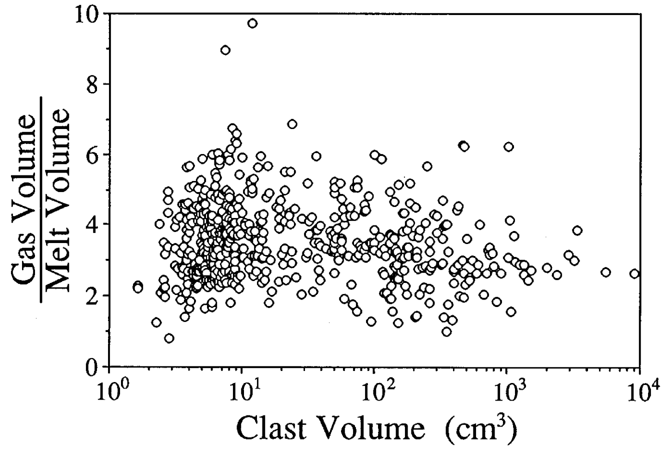

Fig. 3 Variation in V_G/V_L as a function of pumice size. There is no correlation of gas volume ratio with pumice size, indicating that pumice populations of different sizes can be compared. For clarity, only pumices from the rhyodacitic Minoan deposit and the phonlitic Montaña Blanca deposits are shown

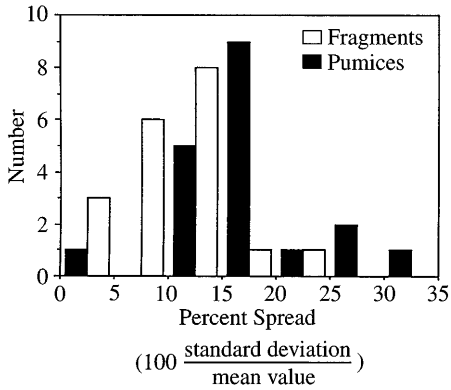

Fig. 4 Histograms of standard deviations (normalized to mean values × 100) of V_G/V_L for populations of fragments from mechanically broken large pumices (*open bars*) and for equalled numbered populations of indivdual pumices (*solid bars*). Both groups are from the Minoan deposit. The greater diversity of the individual pumices indicate that there are larger vesicularity differences between pumices than within them

mice, and Minoan magmas (Table 1) by analyzing glass inclusions in feldspar phenocrysts. Major-element compositions of the inclusions were determined with electron microprobes at Brown University and Université de Paris VI. Water contents were analyzed by secondary ion mass spectrometry (SIMS), using the IMS-3f ion microprobe (Cameca, France) at CRPS, Nancy, France. Sample preparation and analytical techniques are the same as those reported by Gardner et al. (1995b). In addition, we analyzed water contents in five glass standards which were characterized by Fourier transform infrared spectroscopy (FTIR) and manometry, and found excellent agreement between the different techniques. Water contents reported are the highest values found in inclusions which have similar compositions to their host matrix glasses.

Pre-eruptive viscosity was calculated for each of the magmas (Table 1). Because the viscosity of magma changes greatly as it degasses, however, as a result of the strong influence of water content (Shaw 1972), we also calculated the viscosity relevant for postfragmentary evolution, as discussed below.

Gas volume ratios in pumices and erupting magma

Sampling of magma by pumice fragments

We are interested in the properties of the bulk material produced in volcanic eruptions, and a key step is to assess the sample provided by pumices. For example, are pumices produced by one or more mechanisms and, specifically, are pumices generated at the fragmentation level, or is a substantial proportion generated at a later stage? These issues ultimately bear on the question of heterogeneity in the magma, which is discussed after presentation of our data.

The gas volume ratios (V_G/V_L) which we measured were independent of clast size (Fig. 3). A similar lack of variation was observed by Sparks et al. (1981), Walker (1980, 1981a), and Houghton and Wilson (1989), except when clast size approaches that of internal bubbles. None of our samples approach that size. A key point of Fig. 3 is that the spread in our data set, whatever its origin, is not scale-dependent. A potential source for spread in values of V_G/V_L among pumices is breakage of large pumices into fragments during transport and deposition, because these commonly contain spatial gradients in void fraction. In order to assess this, 15 large pumices (8–32 cm) from the Minoan deposit were mechanically broken into 3–14 fragments, their gas volume ratios measured, and the standard deviation for each population (fragments from the same pumice) was computed (Fig. 4). These deviations were compared with those generated by randomly selecting 3–14 smaller individual pumices from the same deposit. The latter showed more spread than the former, although there was considerable overlap. This suggests, on the one

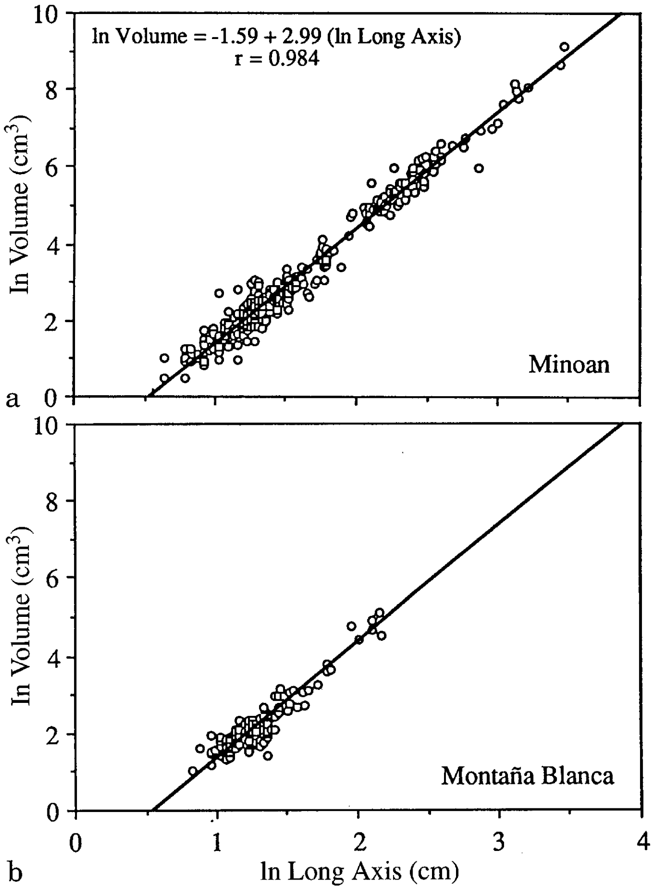

Fig. 5 Variation in long axis of pumices with their volumes for **a** rhyodacitic Minoan pumices and **b** phonolitic Montaña Blanca pumices. Long axis is proportional to volume cubed, as shown by the correlation for the Minoan pumices. This correlation is shown against the Montaña Blanca pumices demonstrating the coherence of other populations to the proportionality, regardless of composition

hand, that a substantial part of the variability in our pumice samples could result from breakage of larger pumices with internal gradients and, hence, makes the origin of these gradients an important issue. On the other hand, Figs. 3 and 4 taken together imply that breakage cannot be the sole explanation for the spreads in the populations which we studied.

Fragments may undergo viscous deformation after fragmentation and before chilling. Anisotropic deformation, such as shear, would generate a systematic dependence of shape on fragment size and magma viscosity. We find, however, that pumice shape is independent of size and composition (Fig. 5), and infer that such deformation was not strongly anisotropic. The most plausible interpretation of the above results is that all of the pumices are produced by the same sequence of mechanisms. We conclude that pumices of any size from a given deposit belong to a coherent population and represent a meaningful sample of the bulk magma involved in these eruptions.

Variations in gas volume ratios in pumices

Overall, V_G/V_L ranges from 0.136 to 13.71, showing that gas volumes differ between Plinian eruptions by two orders of magnitude (Table 2). Indeed, the entire range is even greater when the reticulites ($V_G/V_L = 49$) from the Montaña Blanca deposit are considered. Average V_G/V_L varies between 1.42 and 4.75, indicating that the mean gas volume more than triples between deposits. In individual deposits, the mean values of different populations differ by up to 70%. Even more spectacular, pumice clasts at a given level in a deposit can have gas volume ratios as different as a factor of 35 (Table 2). Indeed, the smallest difference in gas volume in a given level is greater than a factor of 3. Thus, even at a specific time during a Plinian eruption, pumices with very different gas volume ratios are produced.

The pumices sampled come from magmas which range in bulk and matrix-glass composition from basalt to high-silica rhyolite and phonolite (Table 1). These magmas contain 0–43 vol.% crystals and initially ~2–6.5 wt.% water. There are, however, no systematic variations in mean gas volume ratios with glass chemistry, pre-eruptive water content (Fig. 6a), or crystallinity (Fig. 6b). There are weak correlations between compositional variations and the variation in V_G/V_L within samples, with the range in gas volume ratios increasing as magmas become more basic, hotter, dryer, and less crystalline.

In summary, large differences in gas volume occur in Plinian eruptions, whether comparing different eruptions, different times during eruptions, or different pumices at a specific time in an eruption. If pumices quench at the level of fragmentation, then these variations must relate to either compositional differences between erupting magmas or to differences in eruptive dynamics. If, on the other hand, the vesicularity of pumices evolves after fragmenting, then the variations in gas volume reflect this evolution. To investigate these alternatives, we examine below the variations of V_G/V_L in relation to compositional variations, eruptive dynamics, and postfragmentation processes. In the subsequent discussions on the possible influences on V_G/V_L, we have not included the sample from the first gray level of the 79 A.D. Vesuvius deposit, because of possible non-steady-state effects during that phase of the eruption (Appendix). We do show that the sample can be explained by our model for fragmentation and postfragmentary evolution.

Influence of magma composition and eruptive dynamics on gas volume ratios

Several factors have been proposed to lead to variable pumice vesicularity, among them differences in water content, crystallinity, and mass flux of the eruption (Sparks 1978; Carey and Sigurdsson 1987; Sigurdsson et al. 1990; Klug and Cashman 1994a). Low water con-

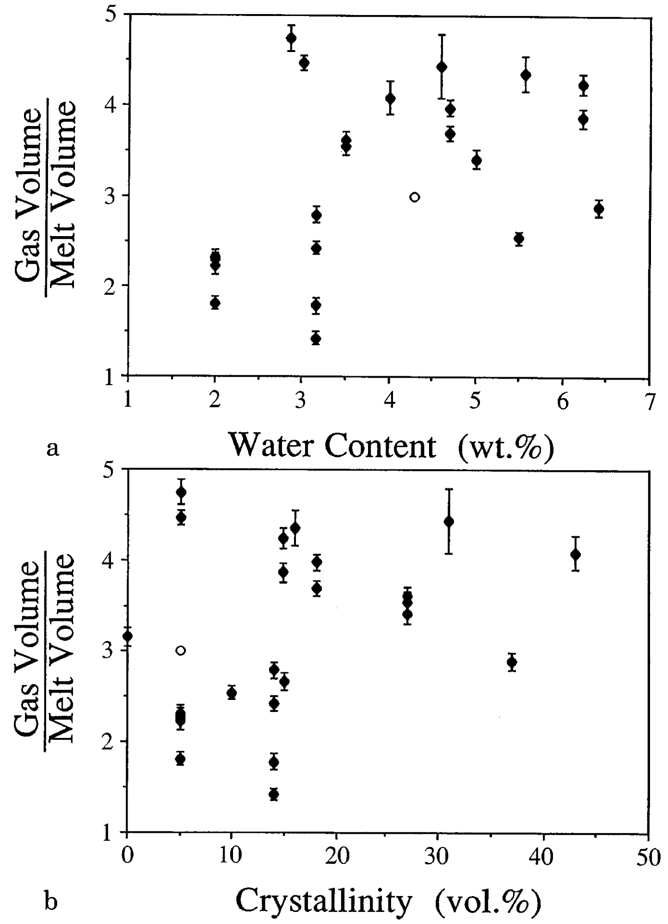

Fig. 6 Variations in V_G/V_L as a function of **a** initial dissolved water content and **b** crystallinity (Table 1). *Error bars* are standard errors of the mean value. Mean V_G/V_L for the Taupo Plinian deposit (*open circle*) is also shown. Data for Taupo are from Houghton and Wilson (1989), Palais and Sigurdsson (1989), and Dunbar et al. (1989a, b)

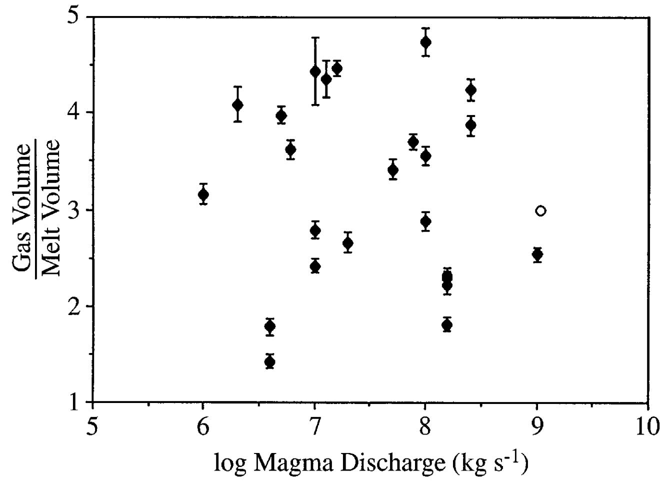

Fig. 7 Variations in V_G/V_L as a function of magma discharge (Table 1). Mean value for the Taupo Plinian deposit is also shown (see Fig. 4). Magma discharge for Taupo is from Carey and Sigurdsson (1989)

tents and high crystallinities are suggested to suppress bubble growth, and thus lower vesicularities. Crystals may also act as nucleation sites for bubbles, so they could in fact enhance vesicularity (Hurwitz and Navon 1994). Variations in mass flux are thought to cause variations in vesicularity, because they may determine the time available for bubbles to grow (Sparks 1978).

We have demonstrated, however, that mean volume ratios do not vary systematically as a function of initial water content (Fig. 6a). This comparison uses average water contents for the magmas, so it might be argued that gas volume variations reflect heterogeneities in water content in magmas. The level of heterogeneity required can be calculated. Assuming that for each sample the pumice with the highest gas volume ratio initially contained the highest water content, and that all pumices in the sample quenched at the same pressure, then we calculate that a >2 wt.% decrease in water content is needed in each sample to explain the lowest observed gas volumes, including those from single levels within deposits. It is unlikely that such differences in water content were present within any of the studied magmas.

We also find no systematic variation in gas volume ratio with crystallinity; pumices containing <10 vol.% crystals are as vesicular as those containing >15 vol.% (Fig. 6b). This is despite a 43 vol.% range in crystallinity. In fact, the average V_G/V_L for the whole data set (3.19) is equal to that of the holohyaline pumices from the Newberry deposit (Table 2). The case of the Newberry deposit shows that gas volume varies greatly even when no crystals are present.

There is also no systematic variation in mean volume ratio with mass discharge rate (Fig. 7). Furthermore, large variations in gas volume occur at discrete levels in deposits; yet, it is implausible that these pumices erupted at significantly different discharges. There is, however, a suggestion that mean V_G/V_L changes with stratigraphic height in deposits (Table 1). In the compositionally homogeneous Minoan and Upper Scoria 1 deposits, mean values are lower at the base of the deposits than at the top, which were erupted at higher intensities. In a more detailed sampling of the Minoan and Bishop tuff Plinian deposits, it is found that vesiculation increases systematically upward in the deposits, which correlates with increased discharges (Houghton and Wilson 1989; Gardner et al. 1991; Thomas et al. 1994). When both composition and discharge change, however, it appears that the effect of composition outweighs that of discharge, as shown by the Middle Pumice deposit in which andesitic pumices are markedly less vesicular than dacitic ones, although the andesitic ones erupted at a higher discharge (Table 1).

The above results indicate that neither crystallinity, nor water content, nor discharge of magma alone control the final gas volumes of pumices. We conclude, therefore, that the large spreads in V_G/V_L do not reflect pre-eruptive heterogeneities in the magmas. We now investigate whether V_G/V_L values result from processes occurring after fragmentation.

Evolution of gas volume ratios after fragmentation

After fragmentation, clasts of vesiculated magma are carried upward in the conduit and cool only when the eruption column enters the atmosphere; they are not quenched instantaneously when fragmentation occurs (see discussion in Thomas et al. 1994). During the time between fragmentation and quenching, several effects can come into play which affect vesicularity. If gas bubbles within a fragment remain isolated from the exterior and retain their gas, they continue to expand as a result of decompression. If the bubbles become interconnected, they lose their gas, and the fragment may collapse as a result of surface-tension forces acting on the contorted walls of the void space (Scherer 1977; Scherer and Bachman 1977). One can therefore envision a complex sequence of expansion and collapse before quenching.

Collapse of permeable magma fragments

When its bubbles are interconnected, a magma fragment is permeable and surface tension forces act to reduce the curvature of the liquid/gas interface. This leads to the closure of void spaces. Evidence for this mechanism may be found in samples with the lowest void fraction. Figure 8 shows two Fontana basaltic pumices from the same stratigraphic horizon. One has $V_G/V_L = 4.69$ and contains nearly spherical bubbles; the other has a much lower vesicularity ($V_G/V_L = 0.472$) and smaller, contorted voids. One may interpret the latter as remnants of interconnected void space which shrank until permeability dropped to insignificant values.

Taking a value of 0.4 N m^{-1} for the coefficient of surface tension (σ_S) for silicate melts (Khitarov et al. 1979; Walker and Mullins 1981; Proussevitch and Kutolin 1986), and assuming that the average bubble size

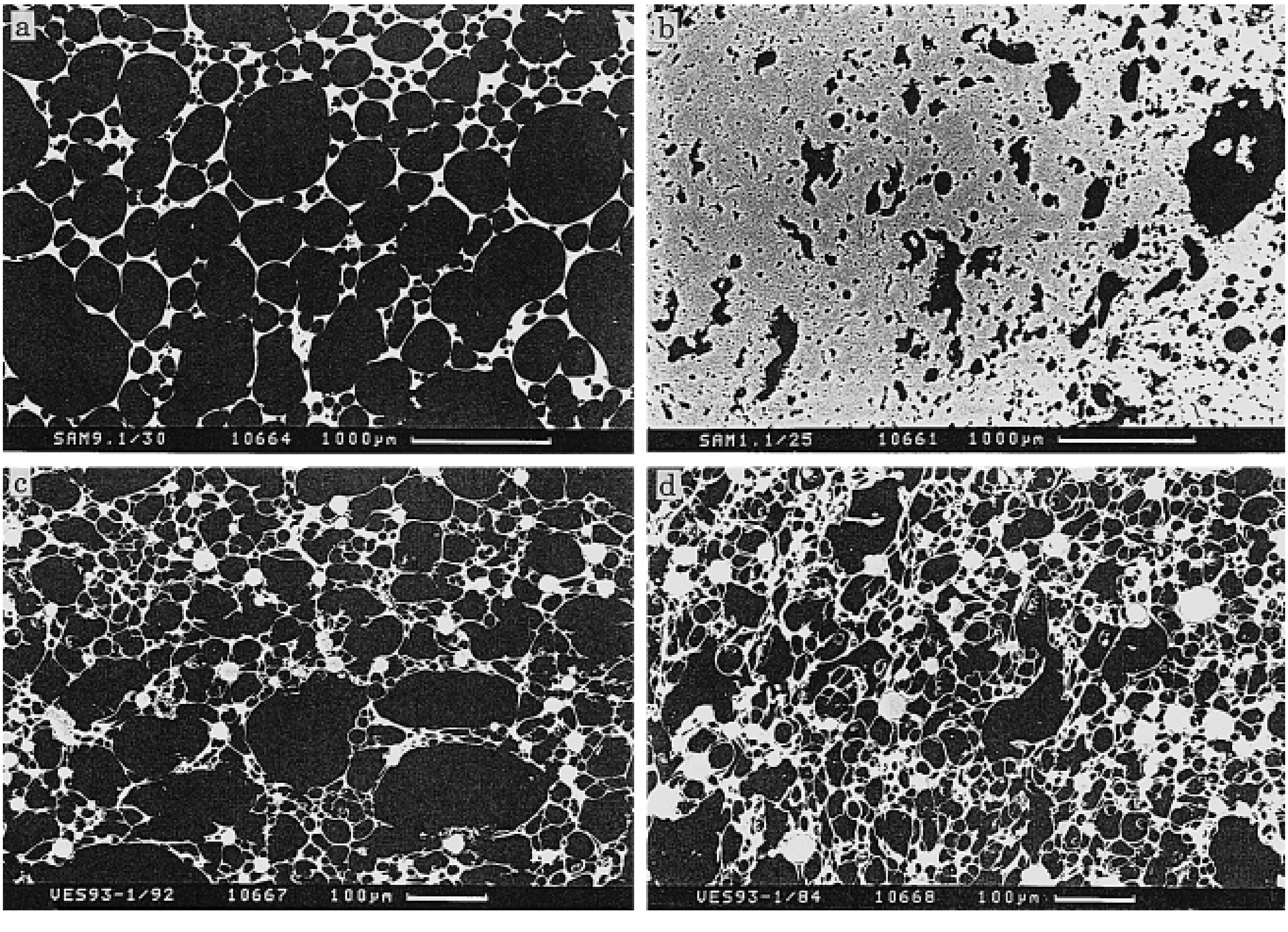

Fig. 8 Digitized back-scattered electron images of **a** Fontana basaltic pumice with $V_G/V_L = 4.69$; **b** Fontana basaltic pumice with $V_G/V_L = 0.472$; **c** Vesuvius phonolitic pumice with $V_G/V_L = 3.89$; **d** Vesuvius phonolitic pumice with $V_G/V_L = 7.84$. *Numbers* at bottom of each image are sample and pumice number (e.g., VES93-1/92), photo number, and scale bar. *White regions* are glass + crystals. The two pumices from each deposit are from the same stratigraphic level

is larger than 10 μm, we find that surface tension stresses do not exceed 4×10^4 Pa. This estimate is much smaller than expected values of overpressure inside bubbles (Thomas et al. 1994). Surface tension forces will therefore be important only when the pressure difference (ΔP) between the interior and exterior of a fragment is small, i.e., after it has degassed significantly. When this is achieved, collapse occurs in a time τ_c approximated by:

$$\tau_c = 3\,\frac{\eta a}{\sigma_S}\left(\frac{\rho_o}{\rho_l}\right)^{1/3} \tag{2}$$

where η is viscosity, a is bubble size, ρ_o density of the vesicular clast, and ρ_l is density of the melt (McKenzie and Shuttleworth 1949; Scherer 1977; Scherer and Bachman 1977). The important relationship is that τ_c is linearly proportional to viscosity. For example, typical values for viscosity and bubble radius for basalt and rhyolite are 10^2 Pa s and 200 μm, and 10^8 Pa s and 50 μm, respectively. These lead to collapse times of approximately 10^{-1} s and 10^4 s.

Expansion of vesicular fragments

There are several pieces of evidence suggesting that pumices have expanded. Highly inflated pumices are found in almost all types of magmas (Houghton and Wilson 1989; Klug and Cashman 1991; Cashman and Mangan 1994; Table 2), including reticulites, with up to 98% vesicularity, like those in the phonolitic Montaña Blanca deposit. Also, at a single stratigraphic horizon in a deposit, one may demonstrate that more vesicular pumices commonly have larger vesicles. Figure 8 shows one such example, from the basal layer of the phonolitic Vesuvius deposit. In the more vesicular pumice, there is a greater number of large vesicles relative to the less vesicular one (Fig. 9). The average shape of vesicles, as measured by the ratio of long axis to short axis, is very similar in the two samples, indicating that the size difference is not an artifact of different shapes. A similar observation was made by Klug and Cashman (1994a) in the 18 May 1980 deposit of Mount St. Helens.

Another observation is that many pumices have internal gradients of vesicularity, in which vesicularity increases from the rim to the center (Fig. 10). These gradients can be interpreted as an interplay between expansion of pumices and their cooling in the atmosphere, as described by Thomas et al. 1994. As a result of air entrainment into the eruption column, cooling of pumices propagates inward from their exteriors. This cooling creates a local viscosity increase in the outer layer, impeding bubble expansion. Eventually, cooling becomes sufficient to prevent dilatation of the whole clast, and the final result is a vesicular interior surrounded by a more compact rim (Fig. 10).

Expansion has been studied in detail by Thomas et al. (1994), and the influence of cooling on expansion has been studied by Kaminski and Jaupart (in preparation). A complete theoretical prediction requires a series of assumptions about fragmentation and flow conditions above fragmentation, and hence is subject to some uncertainty. A simple and reliable way to characterize expansion, however, is by a dimensionless variable B (Thomas et al. 1994):

$$B = \frac{4\eta}{3\tau_e \Delta P_T} \tag{3}$$

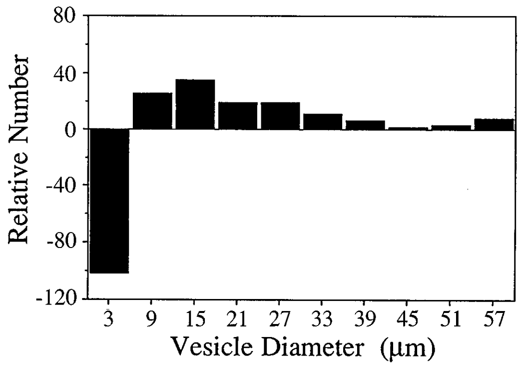

Fig. 9 Difference in number of vesicles per size class between Vesuvius phonolitic pumices (see Fig. 8). Differences equal the number of vesicles in the more vesicular sample (VES93-1/92) minus those in the denser one (VES93-1/84). Several images were analyzed for each pumice, and the numbers measured per size class were normalized to account for the different total number measured. Diameters (in 3D) were calculated from areas by assuming spherical shape. Images were enhanced following the procedure of Klug and Cashman (1994) in which thin, 1-pixel-wide lines (1 pixel = ~0.5 μm) were digitally added to connect vesicle walls so that the image-analysis package could recognize individual vesicles. Vesicles larger than 60 μm were ignored because of random sampling

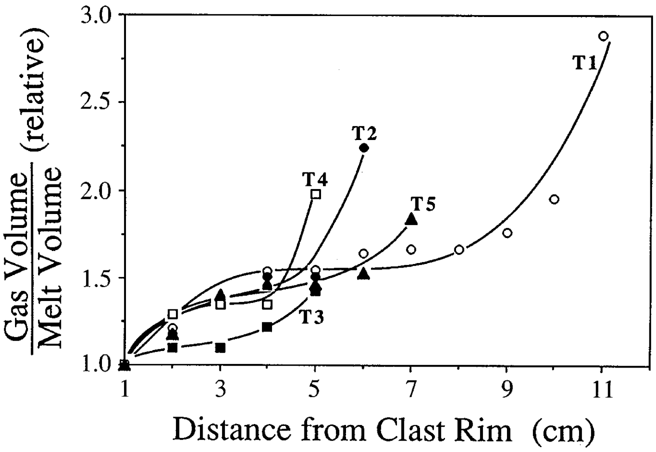

Fig. 10 V_G/V_L as a function of position in large pumice clasts from a phonolitic fall deposit erupted from Teide volcano, Canary Islands. The values of V_G/V_L are for 1-cm-thick cylinders cut from the interior of pumices, 10–22 cm in diameter, and have been normalized to rim value, thus showing the relative increase in gas volume in the interior of pumices

where η is viscosity, τ_e is the time for expansion (before quenching), and ΔP_T is the total pressure drop above the fragmentation level. Viscous retardation becomes significant when B exceeds unity, and prevents expansion completely when B is larger than 10^3. Thus, all else being equal, one may expect that, above a certain viscosity threshold, magma fragments are unaffected by pressure release, whereas below a different viscosity threshold, they expand freely as bubble pressure remains nearly equal to the exterior pressure.

Extents of expansion and collapse in Plinian pumice samples

Observations indicate that some pumices have expanded and collapsed. To demonstrate that these processes are not merely curiosities and are relevant to eruption dynamics, one must show that they affect a large proportion of fragments in a deposit in a systematic manner. Important factors are the time at which gas bubbles become interconnected and the permeability which is achieved. Bubbles may connect within a clast either at the time of fragmentation or later. The fact that bubbles are connected, however, is not sufficient, because gas must escape to prevent expansion. If permeability is large, gases escape rapidly and little expansion occurs, whereas low permeability impedes gas escape and expansion may proceed, increasing vesicularity until some permeability threshold is reached. Once gas has escaped, and the magma fragment has a sufficiently low viscosity, the network of melt surrounding the voids tends to collapse, lowering vesicularity. Additional complexities are linked to the large number of bubbles in a fragment and to the large number of fragments. Bubble connectivity may affect only a restricted number of bubbles in a fragment, and the onset of bubble connectivity may not occur at the same time in all the magma fragments. Such complexities may be responsible for the wide distributions of vesicularity observed, and must be kept in mind when interpreting the data.

Equations (2) and (3) provide a framework for comparing pumices from different eruptions and different magmas. One may think in terms of the different times taken by the processes of expansion and collapse, and compare them to the time available before quenching, which we now estimate. The depth of fragmentation depends on the distribution of dynamic pressure in the conduit flow, which in turn depends on the flow regime and the conduit shape (Wilson et al. 1980). If flow pressures remain close to lithostatic, most magmas are predicted to fragment at shallow depths, typically around 500 m (Wilson et al. 1980; Carey and Sigurdsson 1985). Recent calculations show, however, that once magma vesiculates, flow pressure can deviate dramatically from lithostatic because of viscosity changes due to degassing (Dobran 1992; Sparks et al. 1994). For example, a water-rich rhyolite starting from a 5000-m-deep chamber and ascending in a 50-m-radius cylindrical conduit may fragment at a depth of 4000 m (Sparks et al. 1994). Above the fragmentation level, flow velocities take values within a factor of 2 of 150 m s^{-1} (Wilson et al. 1980; Woods 1988). Thus, magma fragments may spend more than 10 s in the conduit before reaching the vent. After injection into the atmosphere, the temperature in the column decreases rapidly as a result of entrainment of cold air. According to Woods (1988) temperatures should be less than 50% of the initial magmatic values at an altitude of $\sim$5000 m. Such temperatures are well below the glass transition of most common silicate melts (Ryan and Sammis 1981; Neuville et al. 1993; Lejeune 1994). Thus, quenching should be completed at that height. In the eruption column the average velocity in the first 5000 m is $\sim$150 m s^{-1} (Woods 1988), and hence pumices are quenched in less than 35 s after leaving the vent. The total time available between fragmentation and quenching may therefore be as much as 60 s, and is not expected to be less than 10 s.

The amount of time available for collapse is a balance between when ΔP is small and when air chills pumice. Because ΔP must be of the order of 1 bar (see above), pumices are unlikely to start collapsing before they reach the vent. Hence, from Eq. (2) it is clear that collapse cannot affect magmas with viscosities higher than 10^5 Pa s. To characterize the amount of expansion, we add estimates of the total pressure drop after fragmentation (Thomas et al. 1994) and find that quantity ($\tau_e \Delta P_T$) in Eq. (3) varies between 10^6 and 10^9 Pa s. Thus, magmas with viscosities smaller than 10^6 Pa s allow fragments to expand freely, whereas those with viscosities higher than 10^9 Pa s are not expected to expand significantly. The key results here are the large viscosity differences involved, and the clear-cut separation between domains for collapse and for delayed expansion. This allows a general classification which is weakly sensitive to the particulars of any individual eruption, and hence which is suited to the data available herein.

Vesicularity systematics in Plinian eruptions

For a quantitative assessment of the importance of expansion and collapse in magma fragments, we need estimates of the viscosity of magma at and above the fragmentation level. For each deposit we assumed that each fragment evolved from the lowest value of vesicularity in the deposit. We then calculated the pressure decrease needed to achieve that value of vesicularity from the known initial water contents (Table 1) and water solubility laws. From this pressure drop it was then possible to calculate the amount of water left dissolved in the melt. "Partially degassed" viscosities were then calculated using the estimate for residual water and the model of Shaw (1972). The viscosities for our data set encompass almost seven orders of magnitude (Table 2). Although viscosities calculated from the Shaw model must be treated with caution, because the model is based on only a small number of data, the error on individual values of viscosity are likely not to exceed one order of magnitude, which is sufficient for our study, considering the large overall range in values.

Using our viscosity estimates the data may be organized in a coherent and meaningful way. The two most viscous samples (Yn and Bishop) have only 1 in 70 pumices with a gas volume ratio larger than 4 (vesicularity larger than 80%), whereas half of the dacitic Middle Pumice pumices have such high gas volumes (Fig. 11). In contrast, the least viscous, basaltic and andesitic samples are composed mainly of pumices with small gas volume ratios ($V_G/V_L<2$). Mean values of gas volume ratios vary similarly with viscosity; the greatest values are achieved at viscosities between approximately 10^5 and 10^7 Pa s (Table 2). In order to avoid errors resulting from the Shaw model, we consider separately rhyolitic melts, for which compositional variations are small, and hence viscosity variations result mainly from different initial water contents and temperatures. In this restricted and compositionally homogeneous data set, gas volume ratios vary systematically with viscosity (Fig. 12). We also note that samples with very different magma compositions, but with similar values of "degassed" viscosity, such as the phonolites and the dacitic Middle Pumice, lead to similar gas volume ratios (Fig. 13). These facts indicate that viscosity is indeed the main control on pumice vesicularity.

To go further we can separate our data into two categories according to the likelihood of collapse. Samples with viscosities lower than 10^5 Pa s should be affected by collapse and, indeed, we find that their gas volume ratios are systematically smaller than those with viscosities larger than 10^5 Pa s (Figs. 14 and 15). Above this threshold value of viscosity, where we expect that collapse does not occur and hence that magma fragments can only expand, gas volume ratios decrease as viscosity increases. This indicates that expansion is slowed down with increasing efficiency as viscosity gets larger. It is emphasized that the vesicularity variations are as predicted not only in a qualitative way, but also quantitatively. We conclude that the data support our hypothesis that postfragmentation conditions are largely responsible for the values of pumice vesicularity.

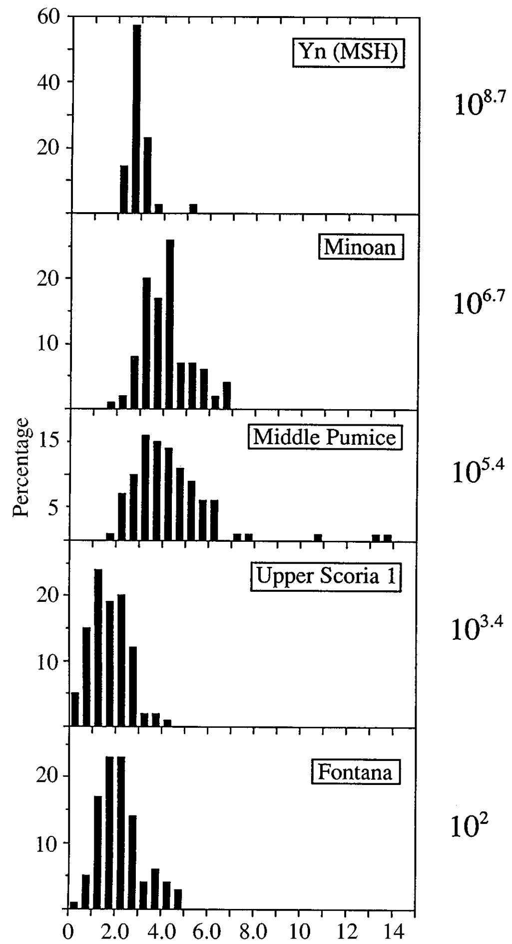

Fig. 11 Variations in V_G/V_L in five different deposits. Note that the ordinate is the percentage of pumices in each division, rather than absolute number. *Numbers* to the right of each histogram is the approximated "partially degassed" viscosity of the magma (Table 2)

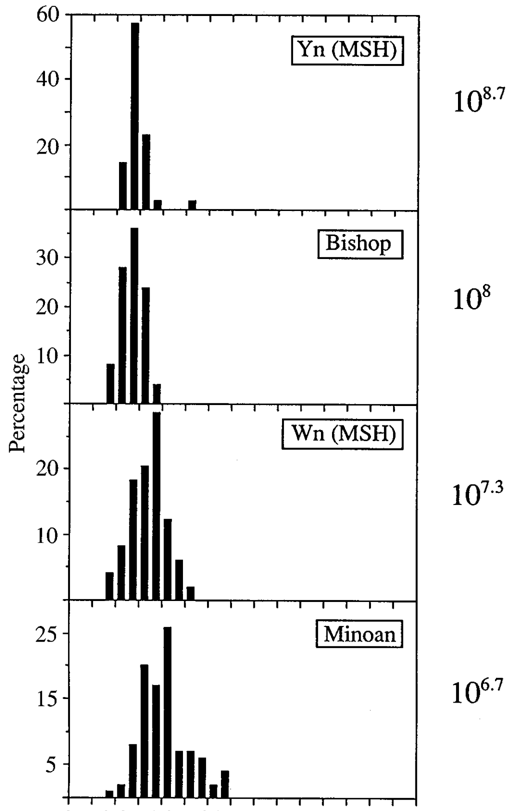

Fig. 12 Variations in V_G/V_L in four deposits with rhyolitic melts (see Fig. 11 for details)

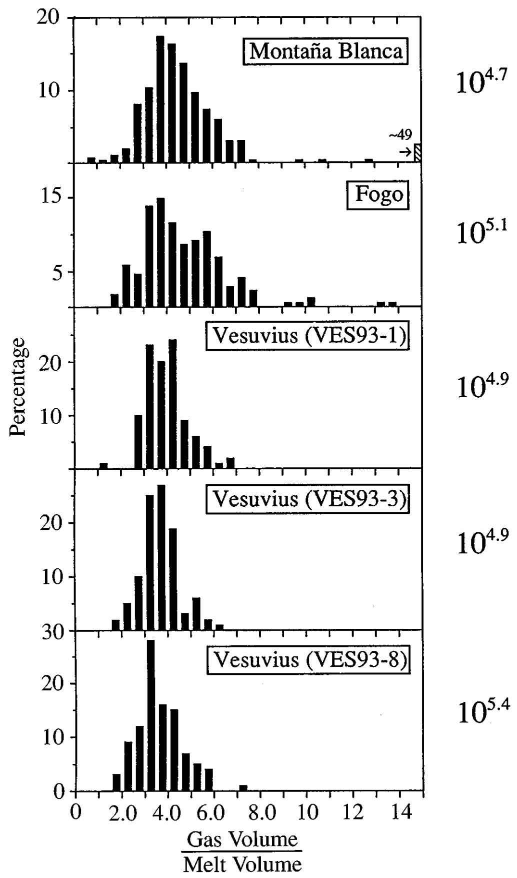

Fig. 13 Variations in V_G/V_L in three deposits with phonolitic melts (see Fig. 11 for details). The three histograms for the Vesuvius deposit are for different stratigraphic levels (Fig. 1d)

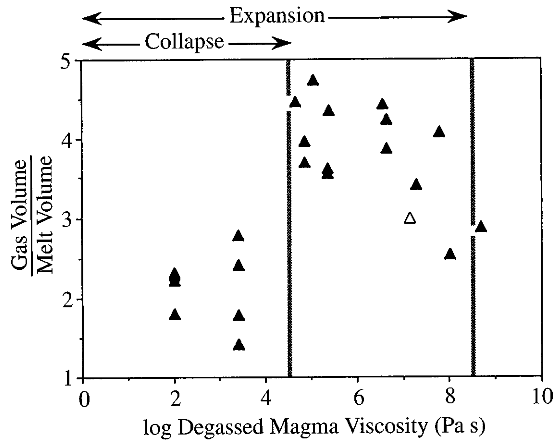

Fig 14 Mean V_G/V_L as a function of partially degassed viscosity. Data are from this study (*filled symbols*) and the Taupo Plinian deposit (*open symbol*). Degassed viscosity for the Taupo magma was calculated using data from sources in Fig. 6. *Shaded lines* delimit regions where expansion and collapse of pumices are expected to strongly affect final V_G/V_L

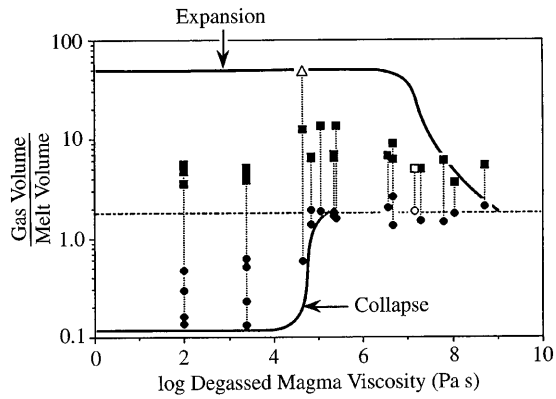

Fig. 15 Maximum (*filled boxes*) and minimum (*filled circles*) V_G/V_L for each population (connected by tie lines) as a function of partially degassed viscosity. Reticulites found in the Montaña Blanca deposit (*open triangle*) and the maximum and minimum ratios in the Taupo Plinian deposit (*open box, open circle*) are also shown (see Fig. 6 for Taupo data). The *upper curve* shows the expected expansion of pumices after 10 s (Thomas et al. 1994). The *lower curve* delineates the range of viscosities where collapse is expected to be important. *Horizontal dot–dash line* shows the average minimum volume ratio at degassed viscosities $\geq 10^5$ Pa s

Timing of bubble connectivity inside magma fragments

Our observations allow constraints on the onset time for bubble connectivity. The basis of the following discussion is that, in all Plinian eruptions, magma fragments experience the same sequence of events, and that the time scales involved are similar. In other words, the inevitable differences in decompression rates and cooling rates which exist between different eruptions are small when compared with the variations of viscosities.

We have seen evidence that fragments expand after fragmentation, but the gas volume ratios are not as large as predicted (Fig. 15). For example, phonolitic and dacitic magmas, whose viscosities are between approximately 10^5 and 10^7 Pa s, should all have expanded to reticulites, yet this is not the case. Reticulites exist, but in small numbers. This indicates that expansion did not proceed to the full extent in most fragments. We suggest that this results from bubbles connecting before quenching, while magma is still liquid. Support for this comes from the fact that low viscosity samples appear to have collapsed, which requires that their bubbles interconnected and became permeable before they were quenched. Further evidence is provided by the dissolved water concentrations in pumice matrix glasses. Blank et al. (1994) found that these concentrations are much smaller than would be deduced from their vesicularities and initial water contents of the pumices. For example, in several pumices from the 1991 eruption of Mount Pinatubo, Philippines, matrix glass contains ~0.42 wt.% water, whereas closed-system degassing to the observed value of vesicularity would lead to water concentrations in excess of 1.2 wt.%. This may be explained by continued degassing after bubbles were connected and the clasts became permeable.

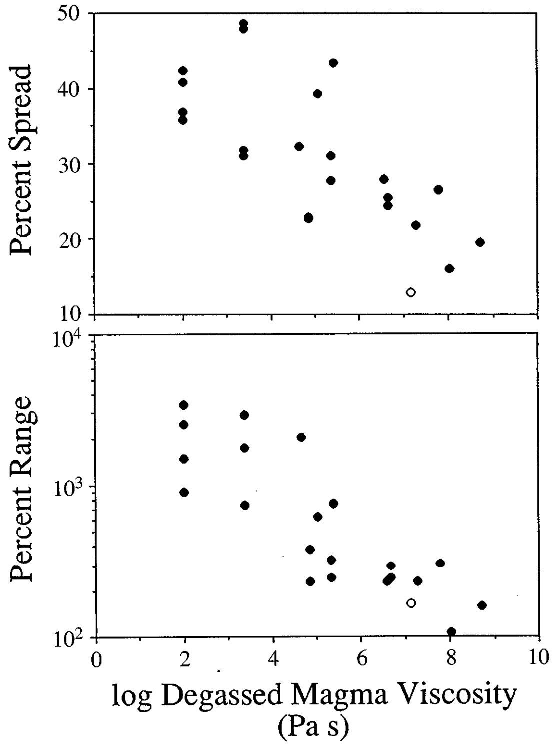

Fig. 16 Variations in percent spread $(100\,\frac{\text{standard deviation}}{\text{mean gas volume ratio}})$ and percent range $[100\,((\frac{\text{maximum gas volume ratio}}{\text{minimum gas volume ratio}})-1)]$ as a function of the partially degassed viscosity of the magma. Data are from this study (*filled circles*) and the Taupo Plinian deposit (*open circle*). Degassed viscosity for the Taupo magma was calculated using data from sources in Fig. 6

Finally, the standard deviation and total range in gas volume ratios increase systematically with decreasing viscosity (Fig. 16). This can be understood by the fact that connectivity is unlikely to occur in all fragments simultaneously in an eruption. In addition, the intensity of expansion increases with lower viscosity and collapse becomes significant below viscosities of 10^5 Pa s. Therefore, given a certain amount of time, the gas volume ratios in less viscous pumices are more likely to be altered. The possibility that bubbles degas at different times helps to explain the distributions of V_G/V_L in the samples (Figs. 11–13).

Discussion

We have shown that the systematic features of our data set support strongly the suggestion that vesicularity is altered after fragmentation. These processes include the expansion of pumice, development of bubble connectivity to form permeable networks, and collapse of fragments as a result of surface tension forces. In light of these results, we now discuss the possible extent of heterogeneities in the magma at the fragmentation level.

Heterogeneities in vesicularity at the fragmentation level

The values of V_G/V_L in a population of pumices are more diverse than the internal gradients in large pumices (Fig. 4). We may deduce that either bubbles are distributed heterogeneously in the magma at the point of fragmentation on a spatial scale larger than the largest pumice sampled (32 cm), or that post-fragmentation processes developed the observed ranges. If large ranges in V_G/V_L were to reflect the state of magma when it fragments, then the implications would have to be recognized. For example, the range in V_G/V_L in the bottom layer of the Minoan deposit (Table 2) would reflect a difference of ~3.7 wt.% in the amount of gas exsolved, if the pressure were constant across the fragmentation level, or a pressure difference of ~200 bar across that level, if the mass fraction of gas were constant. Such an extreme pressure gradient or difference in degassing efficiency seems implausible and implies strongly that the ranges do not reflect the state of the magma when it fragments. Small heterogeneities at the point of fragmentation are not, however, ruled out, because only small differences in pressure or exsolved water content would be required.

We have shown that postfragmentation processes can arguably generate very nearly the entire range of values from a homogeneous starting material. However, one piece of evidence for heterogeneity at fragmentation is that the maximum V_G/V_L value in the Yn deposit of Mount St. Helens cannot be generated by expansion from the minimum value in a reasonable amount of time (Fig. 15). This magma is extremely viscous and the possible extent of expansion is correspondingly limited. In order to corroborate this observation, we obtained data from the 1991 Pinatubo deposit, which is similarly viscous (Blank et al. 1994). We were not able to make a statistically valid study of this example, but did find values which indicate a minimum range for V_G/V_L from 2.7 to 4.0. This range is also larger than might be predicted by expansion alone. We thus conclude that magmas are to some extent heterogeneous with respect to vesicularity when they fragment. Accounting for the effects of expansion, using data from the Yn deposit, suggests that a heterogeneity in V_G/V_L of ~60% existed. This difference is much smaller than the ranges seen in most of the populations studied, however, showing that expansion must be called on to account for the full data set.

The foregoing arguments are based on our observations of pumice clasts, albeit spanning a fairly wide size range. However, a large proportion of ash is produced in explosive eruptions. A central question is whether ash is produced at the same time and by the same mechanism as pumice. If ash is produced mainly at a late stage, e.g., by abrasion of larger particles during transport, then pumices are the best guide to the state of magma at fragmentation. If most ash is produced at the same time as pumice, then it contains information on the fragmentation process. The constant relationship between the sizes and shapes of pumices (Fig. 5) appears to extend to much smaller particles as well, because grain-size distributions are continuous down to sizes of ~ 100 μm and possibly even to 1 μm (Walker 1981b; Hayakawa 1985). In addition, ash which is much larger than individual bubbles does not differ notably from pumices in average density, and hence vesicularity, and is typically similar morphologically to pumice (Walker 1980, 1981b; Talbot 1988). Furthermore, it has been observed that the compositions of glass from pumice and ash are compositionally similar in the same eruptions (Izett 1982; Sarna-Wojcicki et al. 1981, 1987). Such continuous distributions of grain size, vesicularity, and composition are more likely to be generated from relatively homogeneous magma.

In summary, we find evidence for small heterogeneities in V_G/V_L at the time of fragmentation. A possible source of heterogeneity is the presence of gas bubbles in the magma chamber prior to eruption, as has been suggested for the recent eruptions of El Chichon, Nevado del Ruiz, and Pinatubo (Luhr et al. 1984; Sigurdsson et al. 1990; Gerlach et al. 1996). This could also be true in the eruptions which we studied, and has indeed been suggested for the Bishop tuff (Anderson et al. 1989). If present, this gas would expand during the decompression from the chamber to the fragmentation level to produce bubbles presumably larger than those nucleated in the conduit. These larger bubbles may ultimately be included in the pumices, or they may be wholly lost if they form the surfaces upon which the magma breaks up. In the former case we would expect to see heterogeneity on a scale smaller than the pumices, other than that related to expansion, but we do not. In the latter case our proposal below for the vesicularity at fragmentation is an underestimate. We emphasize, however, that almost all of the observed variations can be explained by post-fragmentary processes.

Fragmentation of vesiculated magma

If post-fragmentation processes produce most of the observed spreads in V_G/V_L, do any pumices preserve the state of magma when it fragments? A small proportion of fragments may become permeable at or just after fragmentation and, if their viscosities are $>10^5$ Pa s, they can record fragmentation. In our more viscous samples there is the striking feature of a relatively constant minimum V_G/V_L of 1.78 (± 0.33), corresponding to a vesicularity of 64.0 (± 5) vol.% (Table 2). Even if we only consider samples with ≥ 90 pumices taken from individual levels, the average is 1.76 (± 0.41). In addition, most other values of V_G/V_L can be modeled as having evolved from this minimum value (Fig. 15). This value is constant over four orders of magnitude in viscosity, regardless of crystallinity, initial water content, melt composition, and eruptive intensity. Thus, it reflects a property of the eruptive mechanism, rather than the type of magma involved, and hence it is probably typical of magma when it fragments. The constancy of this minimum V_G/V_L value also suggests that any excess gas present is volumetrically small.

Our overall data set suggests that fragmentation occurs when magma reaches a vesicularity of approximately 64%, yet we have demonstrated that individual fragments can expand to much greater vesicularities without breaking up. Indeed, highly expanded pumices are found in many magmas (Houghton and Wilson 1989; Klug and Cashman 1991; Cashman and Mangan 1994; this study). This implies that a given threshold of V_G/V_L alone is not a sufficient reason for magma to fragment. We can resolve this apparent paradox by considering the type of deformation which a two-phase mixture undergoes. After fragmentation, isolated pumices undergo uniform expansion with a radial velocity field. In the absence of an externally imposed deformation, films between bubbles rupture only when thinned to a critical thickness, which varies between liquids, but is usually approximately 1 μm (Vrij 1966; Princen 1979; Erneux and Davis 1993; Cashman and Mangan 1994). For typical bubbles found in pumices, such thicknesses may be attained by isotropic expansion once vesicularity exceeds 95% (Princen et al. 1980). This is indeed consistent with the production of reticulites, but implies that a different mechanism is needed to fragment the bulk magma. Before fragmenting, the continuous bubbly liquid is being sheared. This shear may cause the coalescence of enough bubbles to rupture the magma, because shear is able to induce film thinning between bubbles. This will occur, however, only when bubbles are in close packing arrangement, which in practice requires a minimum vesicularity of approximately 60 vol.% (Li et al. 1995 and references therein). This minimum vesicularity is consistent with our observations.

The above interpretations can be fitted to some of the recent work which has been done concerning the transitions from an explosive to an effusive eruption regime. Many lava domes are preceded by explosive phases (Heiken and Wohletz 1987). Eichelberger et al. (1986) suggested that when magmas reach vesicularities of around 60 vol.% they become permeable and are able to lose gas to the surrounding rocks. They proposed that if magma retains sufficient gas to reach 75 vol.%, it erupts explosively, whereas the development of a fractured vent funnel could allow magma to degas upon reaching vesicularities of 60–65 vol.% and hence produce a transition to an effusive regime. Jaupart and Allegre (1991) proposed that the transition could occur even if the permeability of the country rocks remains constant, as a result of decreasing overpressure in the chamber. Their reasoning was that as overpressure decreases, so does velocity in the conduit, and hence a given parcel of rising magma has more time to degas. The model of Eichelberger et al. (1986) requires that the values of vesicularity for explosive and effusive eruptions be different. The estimate of

75 vol.% for fragmentation was derived from the analysis of Sparks (1978), and the threshold value of 60–65 vol.% was determined by permeability measurements on vesicular lava flow samples. Recent hydrothermal experiments lend support for this threshold (Westrich and Eichelberger 1994), but a more extensive suite of permeabilty measurements on vesicular clasts suggests that high permeability may be achieved at lower values (Klug and Cashman 1994b).

These various arguments and observations can be brought together in the following consistent picture. The amount of shear that erupting magma experiences is proportional to its velocity of rise. Once bubbles in ascending magma become packed closely and the gas–melt mixture is sheared sufficiently strongly, magma fragments. As the eruption proceeds the chamber overpressure, and hence the rise velocity in the conduit, may decrease. At some point shear is no longer sufficient to fragment the magma, and the bubble connectivity which develops allows gas to escape. The transition from explosive to effusive regimes can therefore be associated with this difference in the response of the mixture to the intensity of shear and hence to the velocity with which vesiculating magma moves in the conduit. The eruptive sequence during the 1980–1986 activity of Mount St. Helens may illustrate this difference. Initially, magma erupted explosively as it was fed through a conduit at velocities of ~ 1 m s^{-1} (Carey and Sigurdsson 1985; Scandone and Malone 1985). Later in the sequence, the domes were fed at rates one to two orders of magnitude slower (Rutherford and Hill 1993). Because the amount of shear is qualitatively correlated with flow rate, it is relatively independent of the erupting magma. Thus, magmas ranging from basalt to high-silica rhyolite can erupt explosively (Table 1).

This study shows that pumices produced in Plinian eruptions are remarkably diverse. The simple framework developed herein accounts for a large number of their characteristics. The key point is that the action of expansion, cooling, bubble connection, and collapse can generate a diverse population from a homogeneous starting material. We have also shown that a small fraction of pumices undergoes little modification after fragmentation, which allows some deductions to be made about fragmentation. We suggest that fragmentation in Plinian eruptions occurs by strong shearing of a mixture with approximately 64% bubbles by volume.

Appendix

Non-steady-state fragmentation of magma: 79 A.D. Vesuvius

In the 79 A.D. Vesuvius deposit, there is a dramatic variation in V_G/V_L just above the level where a marked change of magma composition occurs, from "white" to "gray" (Fig. 1d). Higher in the deposit, V_G/V_L is similar to that before, with the magma composition remaining constant. Carey and Sigurdsson (1987) noted this level of low vesicularity and suggested that it resulted mainly from the lower water content of the gray magma and possibly to its higher discharge and crystallinity. Based on our data set, we suggest that these factors did not solely cause the low vesicularities of the first gray pumices. In particular, the lower and middle gray levels of the deposit erupted at similar discharges and yet have different vesicularities. In addition, neither water content nor crystallinity vary in the gray deposit (Cornell 1987).

Our own framework, where variations in pumice vesicularity result from post-fragmentary processes, cannot fully explain the vesicularity changes seen in the Vesuvius deposit, because the viscosities of partially degassed white and gray magmas are very similar (Table 2). We note, however, that white and upper gray pumices have very similar values of V_G/V_L. More importantly, the ranges in V_G/V_L for all levels are almost identical, including the first gray pumices. We may infer that the low vesicularity of the first gray pumices resulted from differences in the fragmentation process, rather than in gas expansion or bubble connectivity. Indeed, the first gray pumices erupted at a time when eruption conditions were changing rapidly, as seen from the rapid variations in discharge and magma composition. Such unsteady conditions may explain the low values of vesicularity of the lower gray pumices.

The first gray pumices erupted while the eruption went from its initial steady regime with white magma to another regime with gray magma. The white magma had a higher water content than the gray magma and, hence, fragmented at greater depth (Papale and Dobran 1993). The change in magma composition thus ultimately led to a shallower fragmentation level. One effect of this change may be that fragmentation conditions were different during the transition. A simple idea is that the first gray magma fragmented at the same depth and pressure as white magma, leading to less vesicular fragments. With time the eruption evolved toward a new steady state and gray magma was fragmented at smaller depth and pressure, leading to more vesicular pumices. We believe that these transient variations in vesicularity support our model that fragmentation results from the action of shear, rather than that of bubble overpressure.

Acknowledgements Special thanks goes to Dr. Malcolm Rutherford for kindly allowing J. E. G. to use the electron microprobe at Brown University and to Dr. Joseph Devine for assistance with those analyses. The authors also thank Dr. Etienne Deloule for assistance with the ion microprobe analyses. The sample of 174 pumices from the 4600 y.b.p. eruption of Fogo, Azores, was kindly supplied by Dr. R. S. J. Sparks. Elias Kontsikos, Livia Vitelli, and Alain Creusot-Eon are thanked for assistance in the field. Insightful reviews by Kathy Cashman and Bruce Houghton are appreciated and greatly improved the manuscript. This project was partially funded by the EEC "Environment" program, contract number EVSV-CT92-0178. Fieldwork in Nicaragua was funded by the DRCST program of Ministère des Affaires Estrangères, France.

References

Ablay GJ, Ernst GGJ, Marti J, Sparks RSJ (1995) The ~2 ka subplinian eruption of Montaña Blanca, Tenerife. Bull Volcanol 57:337–355

Andersen DJ, Lindsley DH (1988) Internally consistent solution models for Fe–Mg–Mn–Ti oxides: Fe–Ti oxides. Am Mineral 73:714–726

Anderson AT, Newman S, Williams SN, Druitt TH, Skirius C, Stolper E (1989) H_2O, CO_2, Cl, and gas in Plinian and ash-flow Bishop rhyolite. Geology 17:221-225

Barberi F, Bizouard H, Clocchiatti R, Metrich N, Santacroce R, Sbrana A (1981) The Somma–Vesuvius magma chamber: a petrological and volcanological approach. Bull Volcanol 44:295–315

Barberi F, Cioni R, Rosi M, Santacroce R, Sbrana A, Vecci R (1989) Magmatic and phreatomagmatic phases in explosive eruptions of Vesuvius as deduced by grain-size and component analysis of the pyroclastic deposits. J Volcanol Geotherm Res 38:287–307

Blank JG, Gardner JE, Jaupart C, Sharp Z (1994) Degassing and fragmentation histories of erupted magmas: evidence from matrix glasses in pumice (abstract). EOS 75:719

Carey S, Sigurdsson H (1985) The May 18, 1980 eruption of Mount St. Helens, 2. Modeling of dynamics of the plinian phase. J Geophys Res 90:2948–2958

Carey S, Sigurdsson H (1987) Temporal variations in column height and magma discharge rate during the 79 A.D. eruption of Vesuvius. Geol Soc Am Bull 99:303–314

Carey S, Sigurdsson H (1989) The intensity of Plinian eruptions. Bull Volcanol 51:28–40

Carey S, Sparks RSJ (1986) Quantitative models of the fallout and dispersal of tephra from volcanic eruption columns. Bull Volcanol 48:109–125

Carey S, Gardner J, Sigurdsson H (1995) The intensity and magnitude of Holocene Plinian eruptions from Mount St. Helens volcano. J Volcanol Geotherm Res 66:185–202

Carey S, Sigurdsson H, Gardner JE, Criswell W (1990) Variations in column height and magma discharge during the May 18, 1980 eruption of Mount St. Helens. J Volcanol Geotherm Res 43:99–112

Cashman KV, Mangan MT (1994) Physical aspects of magmatic degassing. II. Constraints on vesiculation processes from textural studies of eruptive products. In: Carroll MR, Holloway JR (eds) Volatiles in magmas 30:447–478

Cornell WC (1987) Petrology and ash dispersal studies of products of the Neapolitan volcanic area. PhD thesis, University of Rhode Island, Narragansett, 255 pp

Dobran F (1992) Nonequilibrium flow in volcanic conduits and application to the eruptions of Mount St. Helens on May 18, 1980, and Vesuvius in AD 79. J Volcanol Geotherm Res 49:285–311

Druitt TH, Mellors RA, Pyle DM, Sparks RSJ (1989) Explosive volcanism on Santorini, Greece. Geol Mag 126:95–126

Dunbar N, Kyle PR, Wilson CJN (1989a) Evidence of limited zonation in silicic magma systems, Taupo Volcanic Zone, New Zealand. Geology 17:234–236

Dunbar N, Hervig RL, Kyle PR (1989b) Determination of pre-eruptive H_2O, F and Cl contents of silicic magmas using melt inclusions: examples from the Taupo volcanic center, New Zealand. Bull Volcanol 51:177–184

Eichelberger JC, Carrigan CR, Westrich HR, Price RH (1986) Non-explosive silicic volcanism. Nature 323:598–602

Erneux T, Davis SH (1993) Nonlinear rupture of free films. Phys Fluids A 5:1117–1122

Gardner JE (1993) Compositional diversity in volcanic deposits: implications for processes operating within magma chambers and the withdrawal of magma during explosive Plinian eruptions. PhD thesis, University of Rhode Island, Narragansett, 222 pp

Gardner JE, Sigurdsson H, Carey SN (1991) Eruption dynamics and magma withdrawal during the Plinian phase of the Bishop tuff eruption, Long Valley caldera. J Geophys Res 96:8097–8111

Gardner JE, Carey S, Rutherford MJ, Sigurdsson H (1995a) Petrologic diversity in Mount St. Helens dacites during the last 4000 years: implications for magma mixing. Contrib Mineral Petrol 119:224–238

Gardner JE, Rutherford MJ, Carey S, Sigurdsson H (1995b) Experimental constraints on pre-eruptive water contents and changing magma storage prior to explosive eruptions of Mount St. Helens volcano. Bull Volcanol 57:1–17

Gerlach TM, Westrich HR, Symonds RB (1996) Pre-eruption vapor in magma of the climactic Mount Pinatubo eruption: source of the giant stratospheric sulfur dioxide cloud. In: Punongbayan RS, Newhall CG (eds) The 1991–1992 eruptions of Mount Pinatubo, Philippines, US Geol Surv Prof Pap (in press)

Hayakawa Y (1985) Pyroclastic geology of Towada volcano. Bull Earth Res Inst Univ Tokyo 60:507–592

Heiken G, McCoy F (1984) Caldera development during the Minoan eruption, Thira, Cyclades, Greece. J Geophys Res 89:8441–8462

Heiken G, Wohletz K (1987) Tephra deposits associated with silicic domes and lava flows. In: Fink JH (ed) The emplacement of silicic domes and lava flows. Geol Soc Am Spec Pap 212:55–76

Hildreth EW (1977) The magma chamber of the Bishop tuff: gradients in temperature, pressure and composition. PhD thesis, University of California, Berkeley, 328 pp

Houghton BF, Wilson CJN (1989) A vesicularity index for pyroclastic deposits. Bull Volcanol 51:451–462

Hurwitz S, Navon O (1994) Bubble nucleation in rhyolitic melts: experiments at high pressure, temperature, and water content. Earth Planet Sci Lett 122:267–280

Izett GA (1982) The Bishop ash bed and some compositionally similar ash beds in California, Nevada, and Utah. US Geol Surv Open-File Rep 82–582

Jaupart C, Allègre CJ (1991) Gas content, eruption rate and instabilities of eruption regime in silicic volcanoes. Earth Planet Sci Lett 102:413–429

Kaminski E, Jaupart C (1996) The size distribution of pumice and ash and their constraints on fragmentation (in preparation)

Khitarov NI, Lebedev YB, Dorfman AM, Bagdasarov NS (1979) Effects of temperature, pressure and volatiles on the surface tension of molten basalt. Geochem Int 16:78–86

Klug C, Cashman KV (1991) Effects of vesicle size and shape on the vesicularity of silicic magma fragmentation (abstract). EOS 72:312

Klug C, Cashman KV (1994a) Vesiculation of May 18, 1980, Mount St. Helens magma. Geology 22:468–472

Klug C, Cashman KV (1994b) The development of permeability in pumice (abstract). EOS 75:702

Lejeune A-M (1994) Rhéologie des magmas: influence des cristaux et des bulles en suspension. Thèse de Doctorat, Université Paris VII, Paris, 225 pp

Li X, Zhou H, Pozridikis C (1995) A numerical study of the shearing motion of emulsions and foams. J Fluid Mech 286:379–404

Luhr JF, Carmichael IS, Varekamp JC (1984) The 1982 eruption of El Chicon volcano, Chiapas, Mexico: mineralogy and petrology of the anhydrite-bearing pumices. J Volcanol Geotherm Res 23:69–108

Marsh B (1981) On the crystallinity, probability of occurrence and rheology of lavas and magma. Contrib Mineral Petrol 78:85–98

McKenzie JK, Shuttleworth R (1949) Phenomenological theory of sintering. Proc Phys Soc Lond 62:833–852

Mellors RA, Sparks RSJ (1991) Spatter-rich pyroclastic flow deposits on Santorini, Greece. Bull Volcanol 53:327–342

Neuville DR, Courtial P, Dingwell DB, Richet P (1993) Thermodynamic and rheological properties of rhyolite and andesite melts. Contrib Mineral Petrol 113:572–581

Orsi G, Gallo G, Heiken G, Wohletz K, Yu E, Bonani G (1992) A comprehensive study of pumice formation and dispersal; The Cretaio Tephra of Ischia (Italy). J Volcanol Geotherm Res 53:329–354

Palais JM, Sigurdsson H (1989) Petrologic evidence of volatile emissions from major and pre-historic volcanic eruptions. In: Berger A, Dickinson RE, Kidson JW (eds) Understanding climate change. AGU Geophys Monogr Ser 52:31–56

Papale P, Dobran F (1993) Modeling of the ascent of magma during the Plinian eruption of Vesuvius in AD 79. J Volcanol Geotherm Res 58:101–132

Princen HM (1979) Highly concentrated emulsions: I. Cylindrical systems. J Colloid Interface Sci 71:55–66

Princen HM, Aronson MP, Moser JC (1980) Highly concentrated emulsions. II. Real systems. The effect of film thickness and contact angle on the volume fraction in creamed emulsions. J Colloid Interface Sci 75:246–270

Proussevitch A, Kutolin V (1986) Surface tension of magmatic melts (in Russian). Geol Geophys 9:67–69

Rutherford MJ, Hill PM (1993) Magma ascent rates from amphibole breakdown: an experimental study applied to the 1980–1986 Mount St. Helens eruptions. J Geophys Res 98:19667–19685

Ryan MP, Sammis CG (1981) The glass transition in basalt. J Geophys Res 86:9519–9535

Sarna-Wojcicki AM, Meyer CE, Woodward MJ, Lamothe PJ (1981) Composition of air-fall ash erupted on May 18, May 25, June 12, July 22, and August 7. In: Lipman PW, Mullineaux DR (eds) The 1980 eruptions of Mount St. Helens, Washington. US Geol Surv Prof Pap 1250:667–681

Sarna-Wojcicki AM, Morrison SD, Meyer CE, Hillhouse JW (1987) Correlation of upper Cenozoic tephra layers between sediments of the western United States and eastern Pacific Ocean and comparison with biostratigraphic and magnetostratigraphic age data. Geol Soc Am Bull 98:207–223

Scandone R, Malone SD (1985) Magma supply, magma discharge and readjustment of the feeding system of Mount St. Helens during 1980. J Volcanol Geotherm Res 23:239–262

Scherer GW (1977) Sintering of low-density glasses. I. Theory. J Am Ceram Soc 60:236–239

Scherer GW, Bachman DL (1977) Sintering of low-density glasses. II. Experimental study. J Am Ceram Soc 60:239–246

Shaw HR (1972) Viscosities of magmatic liquids: an empirical method of prediction. Am J Sci 272:870–893

Sherrod DR, MacLeod NS (1979) The last eruptions at Newberry Volcano, central Oregon (abstract). Geol Soc Am Abstr Programs 11:127

Sigurdsson H, Carey S, Devine JD (1989) Assessment of mass, dynamics and environmental effects of the Minoan eruption of Santorini volcano. In: Hardy DA (ed) Thera and the Aegean world III, vol 2. Thera Foundation, London, pp 100–112

Sigurdsson H, Carey S, Cornell W, Pescatore T (1985) The eruption of Vesuvius in AD 79. Natl Geogr Res 1:332–387

Sigurdsson H, Carey S, Palais JH, Devine JD (1990) Pre-eruption compositional gradients and mixing of andesite and dacite magma erupted from Nevado del Ruiz volcano, Columbia in 1985. J Volcanol Geotherm Res 41:127–151

Sparks RSJ (1978) The dynamics of bubble formation and growth in magmas: a review and analysis. J Volcanol Geotherm Res 3:1–37

Sparks RSJ (1986) The dimensions and dynamics of volcanic eruption columns. Bull Volcanol 48:3–16

Sparks RSJ, Wilson L, Sigurdsson H (1981) The pyroclastic deposits of the 1875 eruption of Askja, Iceland. Phil Trans Roy Soc Lond A299:241–273

Sparks RSJ, Barclay J, Jaupart C, Mader HM, Phillips JC (1994) Physical aspects of magmatic degassing. I. Experimental and theoretical constraints on vesiculation. In: Carroll MR, Holloway JR (eds) Volatiles in magmas 30:413–445

Talbot JP (1988) Grain morphology and origins of fine ash deposits from the 180 A.D. Taupo eruption, central North Island, New Zealand. MS thesis, University of Texas, Arlington, 262 pp

Thomas N, Jaupart C, Vergnoille S (1994) On the vesicularity of pumice. J Geophys Res 99:15633–15644

Vrij A (1966) Possible mechanism for the spontaneous rupture of thin, free liquid films. Discuss Faraday Soc 42:23–30

Walker D, Mullins O (1981) Surface tension of natural silicate melts from 1200–1500 °C and implications for melt structure. Contrib Mineral Petrol 76:455–462

Walker GPL (1980) The Taupo pumice: product of the most powerful known (ultraplinian) eruption? J Volcanol Geotherm Res 8:68–84

Walker GPL (1981a) Plinian eruptions and their products. Bull Volcanol 44:223-240

Walker GPL (1981b) Generation and dispersal of fine ash and dust by volcanic eruptions. J Volcanol Geotherm Res 11:81–92

Walker GPL, Crosdale R (1973) Two Plinian-type eruptions in the Azores. J Geol Soc Lond 127:17–55

Westrich HR, Eichelberger JC (1994) Gas transport and bubble collapse in rhyolitic magma: an experimental approach. Bull Volcanol 56:447–458

Williams SN (1983) Plinian airfall deposits of basaltic composition. Geology 11:211–214

Wilson CJN, Houghton BF (1989) Eruptive mechanisms in the Minoan eruption: evidence from pumice vesicularity. In: Hardy DA (ed) Thera and the Aegean world III, vol 2. Thera Foundation, London, pp 122–128

Wilson L, Sparks RSJ, Walker GPL (1980) Explosive volcanic eruptions, IV, The control of magma properties and conduit geometry on eruption column behavior. Geophy J Roy Soc Astrom 63:117–148

Woods AW (1988) The fluid dynamics and thermodynamics of eruption columns. Bull Volcanol 50:169–193